SIMULATION OF A SIMPLE LORENTZ PLASMA WITH A RANDOM DISTRIBUTION OF INDUCTIVELY LOADED DIPOLES

George Merkel

Harry Diamond Laboratories
Washington, D. C.

November 1973

UNCLASSIFIED

Security Classification

AD 775 448

DOCUMENT CONTROL DATA - R & D

(Security classification of title, body of abstract and indexing annotation must be entered when the overall report is classified)

1. ORIGINATING ACTIVITY *(Corporate author)*

Harry Diamond Laboratories
Washington, D.C. 20438

2a. REPORT SECURITY CLASSIFICATION

Unclassified

2b. GROUP

3. REPORT TITLE

SIMULATION OF A SIMPLE LORENTZ PLASMA WITH A RANDOM DISTRIBUTION OF INDUCTIVELY LOADED DIPOLES

4. DESCRIPTIVE NOTES *(Type of report and inclusive dates)*

Technical Report

5. AUTHOR(S) *(First name, middle initial, last name)*

George Merkel

6. REPORT DATE	7a. TOTAL NO. OF PAGES	7b. NO. OF REFS
November 1973	54	26

8a. CONTRACT OR GRANT NO.	9a. ORIGINATOR'S REPORT NUMBER(S)
b. PROJECT NO. DNA Subtask R99QAXEB088 Work Unit 04 MIPR-73-589	HDL-TR-1637
c. AMCMS Code: 691000.22.63516	9b. OTHER REPORT NO(S) *(Any other numbers that may be assigned this report)*
d. HDL Proj: E053E3	

10. DISTRIBUTION STATEMENT

Approved for public release; distribution unlimited

11. SUPPLEMENTARY NOTES	12. SPONSORING MILITARY ACTIVITY
	Defense Nuclear Agency Work Unit Title "Source-Region Coupling"

13 ABSTRACT

The feasibility of simulating a simple Lorentz plasma with an artificial dielectric constructed from a random distribution of inductively loaded dipoles is investigated. Both the differences and similarities between the macroscopic electromagnetic properties of the artificial dielectric and a Lorentz plasma are discussed.

DD FORM 1 NOV 65 1473 REPLACES DD FORM 1473, 1 JAN 64, WHICH IS OBSOLETE FOR ARMY USE.

UNCLASSIFIED

Security Classification

14. KEY WORDS	LINK A		LINK B		LINK C	
	ROLE	WT	ROLE	WT	ROLE	WT
Nuclear Electromagnetic Pulse						
Plasma Simulation						
Artificial Dielectric						
Ionized Air						
Inductively Loaded Dipoles						

MIPR No. 73-589
AMCMS CODE: 691000.22.63516
HDL Proj: E053E3

HDL-TR-1637

SIMULATION OF A SIMPLE LORENTZ PLASMA WITH A RANDOM DISTRIBUTION OF INDUCTIVELY LOADED DIPOLES

by

George Merkel

November 1973

This research was sponsored by the Defense Nuclear Agency under Subtask R99QAXEB088, Work Unit 04, "Source-Region Coupling."

U.S. ARMY MATERIEL COMMAND
HARRY DIAMOND LABORATORIES
WASHINGTON, D.C. 20438

ABSTRACT

The feasibility of simulating a simple Lorentz plasma with an artificial dielectric constructed from a random distribution of inductively loaded dipoles is investigated. Both the differences and similarities between the macroscopic electromagnetic properties of the artificial dielectric and a Lorentz plasma are discussed.

FOREWORD

The work reported herein was sponsored by the Defense Nuclear Agency under Subtask EB-088 and by the In-House Laboratory Independent Research Program. We wish to thank Mr. Edward Greisch for obtaining the experimental data discussed in this report. We would also like to thank Mr. John Dietz for his many helpful suggestions.

CONTENTS

FIGURES

FIGURES

1. INTRODUCTION

The complete simulation of the electromagnetic pulse, EMP, associated with a nuclear burst involves a number of interrelated parameters. The most obvious parameters are the waveform and the magnitude of the EMP. However, if the system being subjected to the nuclear EMP is in a preionized region such as the ionosphere, we would also have to simulate the ionozation or dielectric constant of the medium surrounding the system such as a missile or satellite. In this work we investigate the feasibility of using an artificial dielectric consisting of a random distribution of inductively loaded short dipoles to simulate the macroscopic electromagnetic properties of a simple Lorentz plasma.[1,2]

During the past twenty-five years a number of so-called artificial dielectrics consisting of regularly spaced rods, parallel plates, metal spheres, etc. have been devised to reproduce the essential macroscopic properties of a dielectric. The ordinary artificial dielectric consists of discrete metallic or dielectric particles or lattices of macroscopic size.[3-7] These artificial dielectrics were first actually conceived as large-scale macroscopic models of microscopic crystal lattices. The practical motivation for the development of the first artificial dielectrics was the desire to obtain relatively inexpensive lightweight materials that could be used for microwave and radar lenses. Several of the artificial dielectrics proposed for microwave lenses have the macroscopic electromagnetic properties of a plasma.[2,4,8,9,10]

A review of the literature reveals a number of papers on the plasma simulation properties of artificial dielectrics consisting of a rigid cubic lattice of three-dimensional grids.[2,4,8] Experimental work, reported in the literature, has been done only on two-dimensional grid. lattice structures.[2,8,10] That a periodic grid structure would produce band structure resonances analogous to Bragg scattering has been discussed from a theoretical viewpoint, but has not been experimentally investigated.[11,12,13,14]

The rigid cubic grid lattice structure has the disadvantage of being somewhat unwieldy and difficult to support and fit around an object with curved surfaces. In general, the cubic lattice grid structure lends itself conveniently to simulation of flat, slab-like plasma sheaths.

In this paper we describe another approach to the simulation of a Lorentzian plasma. We propose a granular pellet-like artificial dielectric consisting of a random distribution of styrofoam spheres containing inductively loaded dipoles which can yield macroscopic electromagnetic constitutive relationships similar to those of a plasma.

A Lorentz plasma can be represented from the viewpoint of macroscopic electromagnetic theory, as a lossy dielectric with a complex dielectric constant given by[1,2]

$$\varepsilon_p = \varepsilon_0 \left[1 - \omega_p^2/(\nu^2 + \omega^2) + j\omega_p^2(\nu/\omega)/(\nu^2 + \omega^2)\right], \quad (1)$$

where ε_0 is the dielectric constant of free space, ω is the frequency of the electromagnetic field, ω_p is the plasma frequency, and ν is the collision frequency between electrons and the gas molecules. We propose to simulate this macroscopic dielectric constant with an artificial dielectric consisting of a random distribution of inductively loaded dipoles encased in styrofoam pellets. A schematic drawing of such a dipole is shown in figure 1. The quantities 2ℓ, L, and R are the length, inductance, and resistance of the loaded dipole respectively. As we will show, using simple quasi-static arguments, if the effective inductance ωL is much greater than the effective capacitance of the dipole, the permittivity of a random distribution of inductively loaded dipoles is

$$\varepsilon_p = \varepsilon_0 \left(1 - \frac{\frac{4}{3}\frac{\ell^2}{\varepsilon_0}\frac{N}{L}}{\left(\frac{R}{L}\right)^2 + \omega^2} + j\frac{\frac{4}{3}\frac{\ell^2}{\varepsilon_0}\frac{N}{L}\left(\frac{R}{L}\right)\frac{1}{\omega}}{\left(\frac{R}{L}\right)^2 + \omega^2} \right) \quad (2)$$

where N is the number density of the dipole pellets. One can see by comparing equation (1) with equation (2), that we can simulate a plasma with plasma frequency ω_p and collision frequency ν by setting

$$\frac{4}{3}\frac{\ell^2}{\varepsilon_0}\frac{N}{L} = \omega_p^2 \quad (3)$$

and

$$\frac{R}{L} = \nu. \quad (4)$$

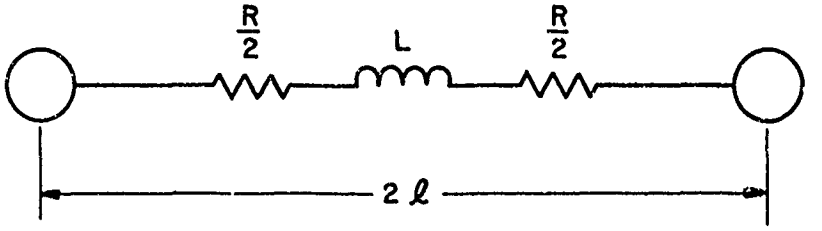

Figure 1. Inductively loaded dipole.

2. THEORETICAL DISCUSSION

2.1 Quasi-Static Approach

We will first approach the problem of our proposed artificial dielectric from a quasi-static viewpoint assuming that the inductive load of the dipole is much larger than the driving point capacitive impedance of a short dipole. In a subsequent section we will explicitly consider the dipole capacitance. First, we discuss the simulation of a tenuous plasma in which the collision frequency between free electrons and molecules, ν, is negligible.

We want to construct an artificial dielectric from a pellet-like medium that has an index of refraction given by[2]

$$n = (1 - \omega_p^2/\omega^2)^{1/2} \tag{5}$$

and an intrinsic impedance given by

$$\eta = \left(\frac{\mu_0}{\varepsilon_p}\right)^{1/2} \tag{6}$$

where ε_p has a frequency dependence of the form[1,2]

$$\varepsilon_p = \varepsilon_0 (1 - \omega_p^2/\omega^2) \tag{7}$$

and where ω_p is the plasma frequency.

In general the index of refraction of an artificial dielectric may be calculated in a manner analogous to that employed in calculating the index of refraction of a molecular medium. Assuming that the random obstacles are not too closely packed so that we do not have to resort to the Clausius-Mossotti relation, the index of refraction is given by[5]

$$n = \left[\varepsilon_1 (1 + N\chi_e/\varepsilon_0)\ \mu_1 (1 + N\chi_m/\mu_0)\right]^{1/2} \tag{8}$$

where

N = Number of scattering obstacles per unit volume,

χ_e = Electric polarizability of a scattering obstacle,

χ_m = Magnetic polarizability of a scattering obstacle,

ε_1 = 1 (for styrofoam),

μ_1 = 1 (for styrofoam),

ϵ_0 = permittivity of free space,

μ_0 = permeability of free space.

From equations (5) and (8) we see that in order to achieve our goal we need an artificial dielectric constructed from obstacles that have a negative electric polarizability, χ_e. If the artificial dielectric is to simulate a plasma over a spectrum of frequencies, the value of χ_e must also be inversely proportional to the frequency squared. We would also like the value of the magnetic polarizability of the embedded obstacles, χ_m, to be small or, if possible, zero.

A promising candidate for a scattering obstacle is an inductively loaded electric dipole. Consider the very idealized inductively loaded dipole schematically shown in figure 2. Let an electric field E be applied parallel to the line between two spheres separated by the distance 2ℓ. The field E then establishes a voltage $V=2\ell E\, e^{j\omega t}$ between the spheres. Assume that inductance between the two spheres is L, and also assume that $L\omega >> 1/\omega C$ where C is the capacitance between the two spheres. Since we are dealing with a time harmonic field assume that the charge accumulated on the dipole spheres is given by

$$q = Qe^{j\omega t} \tag{9}$$

then

$$2\ell E\, e^{j\omega t} = L\frac{d^2q}{dt^2}$$

$$= LQ(-\omega^2)e^{j\omega t}$$

such that

$$Q = -2\ell E/L\omega^2$$

or

$$q = -2\ell E\, e^{j\omega t}/L\omega^2. \tag{10}$$

The dipole moment of the inductive dipole in figure 2 is then

$$p = 2\ell q = -4\ell^2 E\, e^{j\omega t}/L\omega^2$$

or

$$p = \chi_e E\, e^{j\omega t} \tag{11}$$

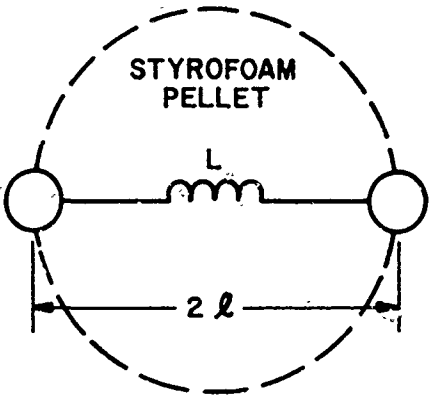

Figure 2. Lossless inductively loaded dipole.

The lossless dipole corresponds to a collisionless plasma.

where

$$\chi_e = -4\ell^2/L\omega^2. \tag{12}$$

If we have a random distribution of dipoles, we must, naturally, consider the various orientations that the dipoles can assume. As shown in figure 3 let the E field be in the Z direction. For every random dipole direction θ, we have an equally probable direction $-\theta$. We can therefore pair all the dipoles oriented in the $+\theta$ direction with dipoles oriented in the $-\theta$ direction. The resultant effective dipole moment for a dipole is

$$p(\theta) = -2 \cos\theta \, (\ell \, 2\ell \cos\theta) \, E \, e^{j\omega t}/L\omega^2.$$

The average value for a random distribution of directions, p_{av}, is then

$$p_{av} = \int_0^{\pi/2} -4 \cos^2\theta (\ell^2 E \, e^{j\omega t}/L\omega^2) 2\pi \sin\theta \, d\theta \Big/ 2 \int_0^{\pi/2} 2\pi \sin\theta \, d\theta$$

$$= \frac{1}{3} p = -4\ell^2 E \, e^{j\omega t}/3L\omega^2.$$

Therefore, we have

$$\chi_{eav} = -4\ell^2/3L\omega^2. \tag{13}$$

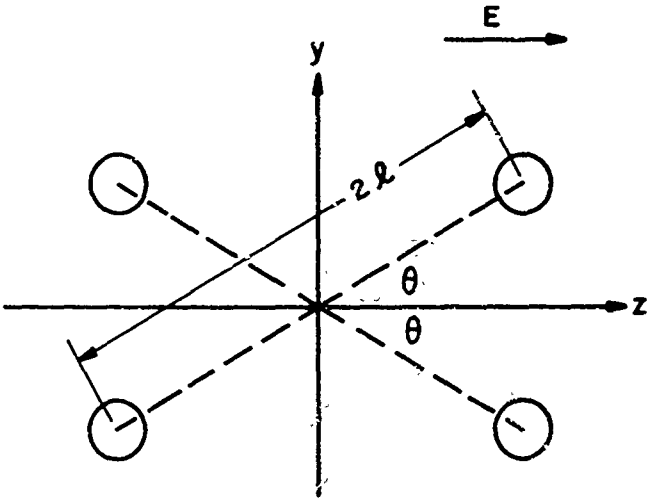

Figure 5. Two dipoles oriented in the θ and -θ directions. The y components of the two dipoles cancel.

Now assuming that $\chi_{mav} = 0$, the index of refraction of the artificial dielectric would be

$$n = \left[1 \left(1 - 4N\ell^2/3\varepsilon_0 L\omega^2\right)_1 \right]^{1/2}$$

and the intrinsic impedance would be

$$\eta = \left[\mu_0/\varepsilon_0(1 - 4N\ell^2/3\varepsilon_0 L\omega^2)\right]^{1/2}$$

In the case of tenuous plasma (ionized high-altitude air) we have an index of refraction given by

$$n = (1 - Ne^2/\varepsilon_0 m\omega^2)^{1/2} = (1 - 3.18\cdot10^9 N/\omega^2)^{1/2} \qquad (14)$$

where N is the electron density in cm^{-3}, m is the electron mass, and e is the electron charge. Therefore, if we want to simulate a tenuous plasma corresponding to electron density N, we can determine the length 2ℓ and the inductance L of our inductively loaded dipoles with the relation

$$\frac{N\ell^2}{\varepsilon_0 L} = \frac{3}{4}\frac{Ne^2}{\varepsilon_0 m} = 2.39\cdot10^9 N \text{ sec}^{-2}$$

or

$$\frac{N\ell^2}{L} = 2.11 \cdot 10^{-2} N \text{ sec}^{-2} \text{ F/m} \qquad (15)$$

where N is the density of artificial dielectric dipoles in meter^{-3}, ℓ is in meters, and L is in henrys.

Next, we note that by introducing a resistance into our dipole we can simulate the imaginary part of the index of refraction that arises because of the collisions, ν, per second between the plasma electrons and the atmospheric molecules. Figure 1 shows that the voltage between the dipole spheres is

$$2\ell E\, e^{j\omega t} = L \frac{d^2q}{dt^2} + R \frac{dq}{dt}$$

where as before we assume $L\omega >> 1/C\omega$. Again, we can assume that the charge on the capacitance between the two spheres varies as

$$q = Q\, e^{j\omega t}.$$

Then

$$2\ell E\, e^{j\omega t} = LQ(-\omega^2)e^{j\omega t} + RQj\omega\, e^{j\omega t}$$

and

$$Q = -2\ell E/(L\omega^2 - jR\omega)$$

or

$$q = -2\ell E\, e^{j\omega t}/(L\omega^2 - jR\omega).$$

The dipole moment along the axis of the inductive dipole in figure 1 is then

$$p = 2\ell q = -4\ell^2 E\, e^{j\omega t}/(L\omega^2 - jR\omega).$$

We see by analogy with the purely inductive dipole

$$p_{av} = \frac{1}{3} p = -4\ell^2 E\, e^{j\omega t}/3(L\omega^2 - jR\omega).$$

Therefore, we have

$$\chi_{eav} = -4\ell^2/3(L\omega^2 - jR\omega) \tag{16}$$

and

$$\varepsilon_p = \varepsilon_0 \left[1 - 4\ell^2 N/3\varepsilon_0 L\omega^2(1 - jR/\omega L)\right] \tag{17}$$

$$= \varepsilon_0 \left(1 - \frac{\frac{4}{3}\frac{\ell^2 N}{\varepsilon_0 L}}{\left(\frac{R}{L}\right)^2 + \omega^2} + j \frac{\frac{4}{3}\frac{\ell^2 N}{\varepsilon_0 L}\left(\frac{R}{L}\right)\frac{1}{\omega}}{\left(\frac{R}{L}\right)^2 + \omega^2} \right). \tag{18}$$

Finally, we note that if equations (3) and (4) are satisfied, we have a one to one correspondence between equations (1) and (18).

2.2 Explicit Consideration of Dipole Capacitance

Up to this point we have assumed that the inductance used to load the short dipole dominated the behavior of the dipole. We will now examine this assumption in more detail. The arguments presented here are basically due to Harrington.[15] Consider two short dipole antennas as shown in figure 4. Antenna 1 is excited by a current source I_1; antenna 2 is loaded at its center with an impedance Z_L. The currents and voltages of the two dipoles can be related by the standard impedances of a two-port network:

$$\begin{aligned} V_1 &= Z_{11} I_1 - Z_{12} I_2 \\ V_2 &= Z_{21} I_1 - Z_{22} I_2. \end{aligned} \tag{19}$$

The voltage V can be expressed in terms of Z_L and I_2: $V_2 = Z_L I_2$. Then we can express the current passing through the load Z_L in terms of the current source driving antenna 1; the transfer impedance Z_{21}; the driving point impedance of antenna Z, Z_{22}; and the load impedance, Z_L:

$$I_2 = \frac{Z_{21} I_1}{(Z_L + Z_{22})}. \tag{20}$$

We next make use of the reaction concept, first introduced by Rumsey.[16,17] Rumsey defined reaction of field a on the source b, {a,b}, with the following integral:

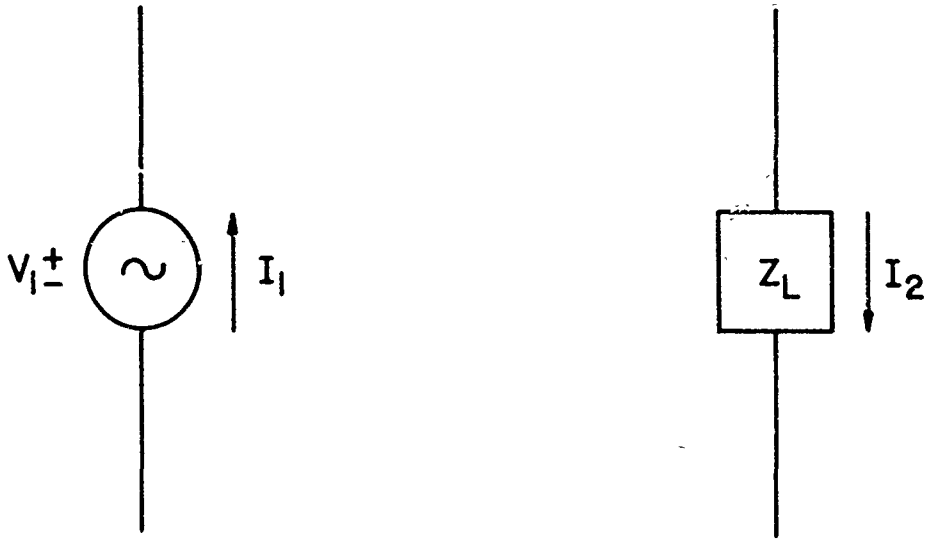

$$V_1 = Z_{11} I_1 - Z_{12} I_2$$

$$V_2 = Z_{21} I_1 - Z_{22} I_2$$

Figure 4. Two short dipole antennas.

$$\{a,b\} = \iiint (\underline{E}^a \cdot \underline{J}^b - \underline{H}^a \cdot \underline{M}^b)\, dv$$

where $\underline{J}^b$ is the electric current density of source b and $\underline{M}^b$ is the magnetic current density of source b. In this notation the reciprocity theorem is:

$$\{a,b\} = \{b,a\}.$$

For a current source I_b, we can obtain

$$\{a,b\} = \int \underline{E}^a \cdot \underline{I}^b \, d\ell = I^b \int \underline{E}^a \cdot d\underline{\ell} = - V^a I^b. \qquad (21)$$

The transfer impedance in equation (19) is defined by

$$Z_{ij} = V_{ij}/I_j$$

where V_{ij} is the voltage at terminal i produced by the current source at terminal j. In equation (21) we indicate that

$$\{j,i\} = - V_{ij} I_i,$$

therefore, we obtain by eliminating V_{ij} and using the reciprocity theorem

$$Z_{ij} = -\frac{1}{I_i I_j} \iint E_i \, J_j \, ds. \tag{22}$$

We next remove dipole number 1 to minus infinity so that the electric field, E_1, at dipole number 2 is a plane wave. King[18] shows that for a short dipole of length B, i.e. for $(\pi/\lambda)\, B < 1/2$, we can assume an induced current distribution on dipole 2 of the form:

$$I_2^1 (z) = I_2\left(1 - \frac{2}{B} |z|\right). \tag{23}$$

Equation (22) then yields:

$$Z_{12} = \frac{E_1 B}{2 I_1} = Z_{21} \tag{24}$$

and from equation (20) we obtain:

$$I_2 = \frac{Z_{21}\, I_1}{(Z_L + Z_{22})} = \frac{E_1 B}{2(Z_L + Z_{22})}.$$

Equation (23) then can be expressed as

$$I_2^1(z) = \frac{E_1 B}{2(Z_L + Z_{22})} \left(1 - \frac{2}{B} |z|\right). \tag{25}$$

The conservation of charge along dipole number 2 can be expressed as

$$\frac{d\, I_2^1(z)}{dz} + j\, \omega\, q(z) = 0, \tag{26}$$

where q(z) is now the charge per unit length, and therefore the charge distribution along dipole 2 is:

$$q(z) = \frac{j}{\omega} \frac{d\, I_2^1(z)}{dz}. \tag{27}$$

The dipole moment along antenna 2, p, is given by the following integral:

$$p = \int_{-\frac{B}{2}}^{\frac{B}{2}} q(z)\, z\, dz. \tag{28}$$

Expressions (25), (26), and (28) then yield:

$$p = \frac{-j\ E_1\ B^2}{4\omega(j\ \omega L + Z_{22})}. \tag{29}$$

If we allow χ to be the polarizability of the dipole we have:

$$p = E \cdot \chi \tag{30}$$

or

$$\chi = \frac{-j\ B^2}{4\omega\ (j\omega L + Z_{22})}. \tag{31}$$

Equation (31) is essentially the same as the result we obtained with the simple quasi-static model, except for the presence of the driving point impedance Z_{22} in the denominator. (The factor 4 in the denominator occurs because we have not capacitively end-loaded the dipole as in figure 1.)

King[19,20] derives a value for the impedance Z_{22} of a short dipole:

$$Z_{22} = \frac{\eta}{2\pi}\left[\frac{(\frac{\omega}{c})^2\ B^2}{12} - j\ \frac{4\ln\ (\frac{B}{A}) - 6.78}{(\frac{\omega}{c})b}\right]. \tag{32}$$

Here η is the impedance of free space, 120 $\pi\Omega$, B is the length of the dipole, and A is the dipole radius.

Up to this point we have considered the incident electric field E, to be parallel to the short inductively-loaded dipole. Of course, the current and charge distribution along the dipole is a function of the orientation of the receiving antenna with respect to the surface of constant phase of the incident electric field. King[19] indicates that for a short receiving antenna (with a triangular current distribution) the projection of the electric field onto the antenna, multiplied by the actual half length of the antenna gives the emf of the equivalent circuit. That is equation (24) is modified to

$$Z_{12} = Z_{21} = \frac{E_1 B}{I_1 2} \cos\ \theta \tag{33}$$

where θ is the angle between the incident electric field vector and the antenna. For example, $\theta = 0^\circ$ when the antenna lies in the surface of constant phase. We can now use the same orientation arguments that we used in the development of our quasi-static model which

ignored the self impedance Z_{22}. If we wish to calculate the polarization in the direction of the incident electric field when the E_1 vector is not parallel to the dipole, we must introduce another cos θ and integrate over all directions. Therefore, as before

$$p_{av} = \frac{1}{3} p$$

and

$$p_{av} = \chi_{av} E$$

or

$$\chi_{av} = \frac{-j B^2}{12\omega(j\omega L + Z_{22})}. \tag{34}$$

If we set $Z_{22} = 0$, $B = 2\ell$, and end-load the dipole so that the current distribution is uniform and not triangular, we obtain the same result as given by equation (13).[18]

The appearance of Z_{22} in the denominator of expression (34) is inconsistent with our desire to model a simple Lorentzian plasma. Specifically, when the frequency is such that

$$\omega L = \left[\frac{4\ln(\frac{B}{A}) - 6.78}{(\frac{\omega}{c}) B}\right] (\frac{\eta}{2\pi}) \tag{35}$$

the artificial dielectric will pass through a resonance. We can only use the inductively-loaded dipoles to simulate a plasma if $\omega L >> Z_{22}$. We will discuss the effect of Z_{22} in a subsequent section. An insight into the limitations imposed by the dipole self-impedance can be obtained by calculating χ_{av} for some realistic frequencies and dipole parameters.

2.3 Mutually Perpendicular Dipole Scatterers

Our arguments presented so far assumed that the distance between the inductively-loaded dipoles is great enough so that their interaction can be neglected. The use of equation (8) is based on the assumption of negligible interaction between scattering objects. A way of increasing the value of N in (8) by a factor of 3 and still not violate the assumption of negligible interaction of neighboring scatterers is to construct each scatterer out of three mutually-perpendicular inductively-loaded dipoles. By using essentially quasi-static arguments it is easy to see that three mutually-perpendicular dipoles with a common center point do not interact.

Consider just two perpendicular dipoles as shown in figure 5. By symmetry the current distribution along the two arms of dipole 1 is symmetrical and equal in magnitude. Therefore, the charge distribution along the opposite arms is equal in magnitude but of opposite sign. Using a static argument the electric field produced by the charge distribution along dipole 1 is seen to be perpendicular to the direction of dipole 2. The dipoles therefore do not interact. Similar reasoning applies to a dipole that is mutually perpendicular to dipoles 1 and 2 and centered at the intersection of dipoles 1 and 2. These quasi-static arguments are consistent with the more rigorous arguments presented for skew-angled dipoles by Richmond.[21] If we substitute three mutually-perpendicular dipoles for the single randomly-distributed dipoles we simply multiply the average value of the polarizability given in equation (34) by 3 and obtain

$$\chi_{av3} = \frac{-j B^2}{4\omega(j\omega L + Z_{22})}. \tag{36}$$

By constructing our scatterers out of three mutually-perpendicular inductively-loaded dipoles we accomplish more than simply increasing the number of scatterers by three: the polarizability of the scattering centers is made to be independent of scatterer orientation. To be specific, the scatterer, consisting of three identical, short, mutually-perpendicular dipoles centered at the origin with a dipole along each axis, can be described with the following simple dyadic:

$$\underline{\underline{\chi}} = \chi (\hat{i}\,\hat{i} + \hat{j}\,\hat{j} + \hat{k}\,\hat{k}) = \chi \underline{\underline{I}}.$$

The dipole moment induced by an arbitrary field $\vec{E}$ is then

$$\begin{aligned} \vec{p} &= \underline{\underline{\chi}} \cdot \vec{E} \\ &= \underline{\underline{\chi}} \cdot E (\hat{i} \sin\theta \cos\phi + \hat{j} \sin\theta \sin\phi + \hat{k} \cos\theta) \\ &= \chi E (\hat{i} \sin\theta \cos\phi + \hat{j} \sin\theta \sin\phi + \hat{k} \cos\theta) \end{aligned} \tag{37}$$

but $(\sin\theta \cos\phi)^2 + (\sin\theta \sin\phi)^2 + \cos^2\theta = 1$. Therefore, the magnitude of the dipole moment is α E and its direction is in the direction of the electric field regardless of the orientation of the scatterer.

In order to gain insight into the foregoing result we can consider a relatively simple situation in more detail. Figure 6 illustrates two perpendicular inductively-loaded dipoles in the plane of the page. Let the $\vec{E}$ vector of the incident plane wave also be in the plane of the page. The third dipole is perpendicular to the plane of the page, and therefore is perpendicular to the $\vec{E}$ vector and does not interact with the E field. As shown in the figure, the Poynting vector $\vec{S}$ of the incident plane wave is also in the plane of the page. The voltage developed across the load of dipole number 1 is then proportional to E cos θ and the separation of

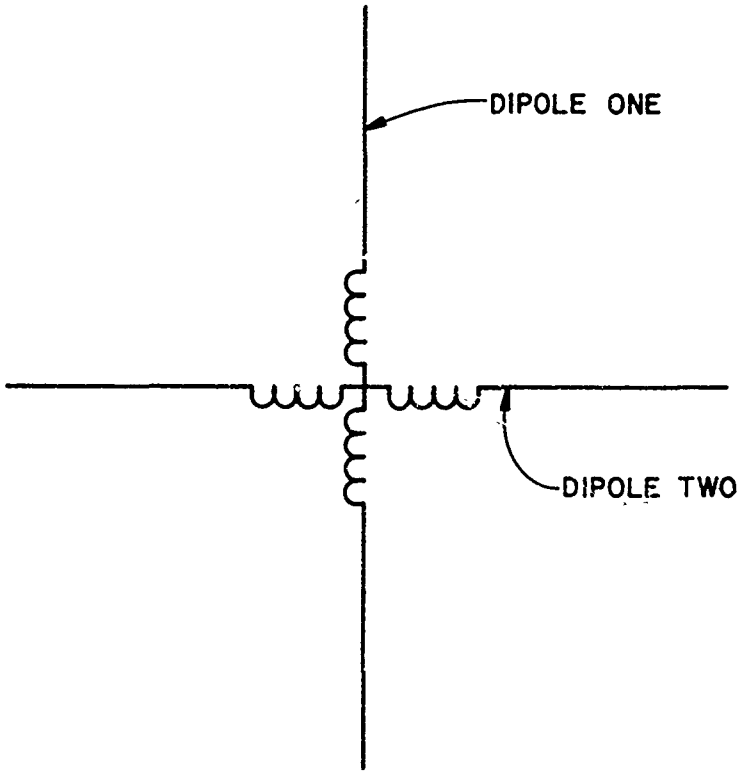

Figure 5. Two perpendicular inductively-loaded dipoles do not interact.

charge on dipole number 1 in the direction of the incident $\vec{E}$ vector is proportional to $\cos^2\theta$, that is $p_{1,E||} = K \cos^2\theta$. A corresponding argument (see fig. 7) leads to the conclusion that the dipole moment of dipole number 2 in the direction of the incident field $\vec{E}$ is given by $p_{2,E||} = K \sin^2\theta$. The total dipole moment in the direction of the vector E of dipoles 1 and 2 is, therefore, given by

$$p_{E||} = p_{1,E||} + p_{2,E||} = K \cos^2\theta + K \sin^2\theta \qquad (38)$$

$$= K = \frac{- j B^2 E}{4\omega(j\omega L + Z_{22})}.$$

Let us now consider the polarization perpendicular to the $\vec{E}$ vector. As shown in figure 8 the voltage developed across the load on dipole 1 is proportional to E cos θ and the dipole moment perpendicular to the E field or parallel to the S vector is $p_{1,E1} = - K \cos\theta \sin\theta$. As shown in figure 7, since the voltage across the load on dipole 2 is proportional to E sin θ, the dipole moment component of dipole two perpendicular to the incident field is

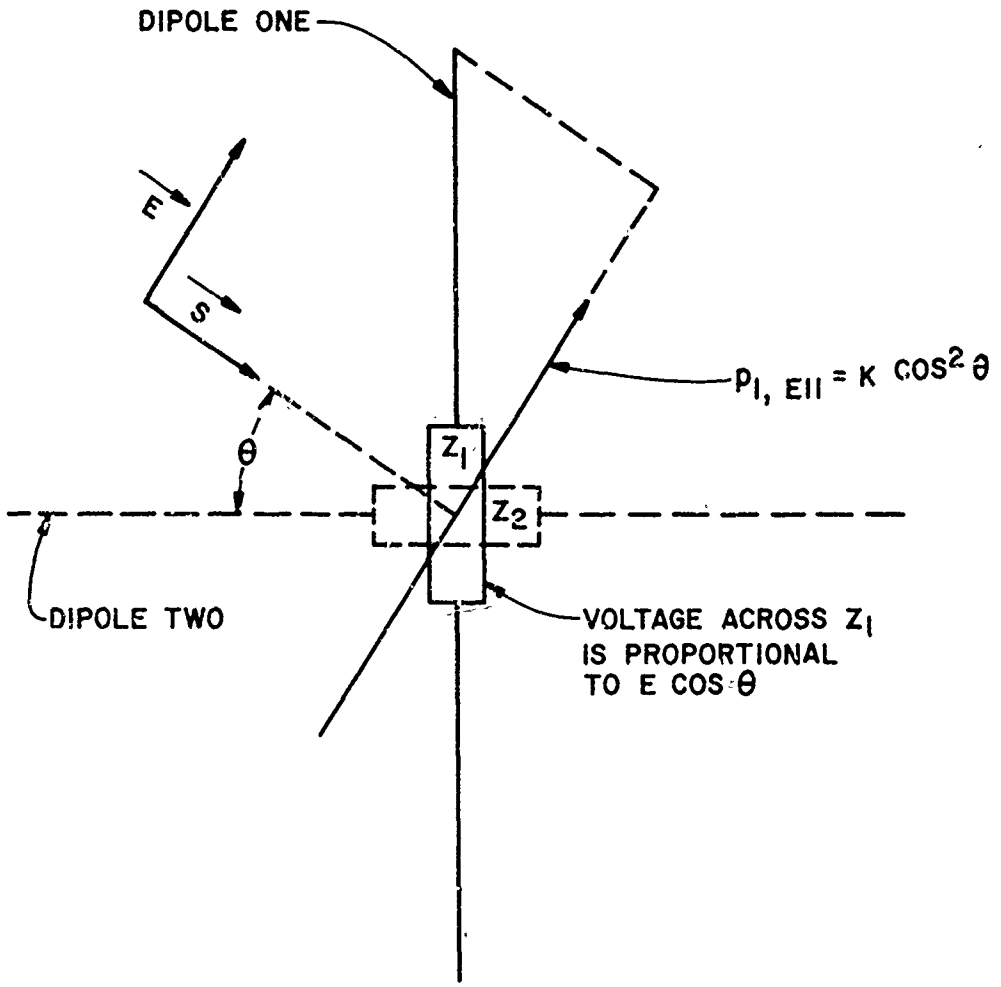

Figure 6. The vector $p_{1,E11}$ is the dipole moment component of dipole 1 that is parallel to the incident electric field.

$$p_{2,E1} = K \sin\theta \cos\theta.$$

So for the total polarization perpendicular to $\vec{E}$ we have

$$\begin{aligned} p_{1E} &= p_{1,E1} + p_{2,E1} \\ &= K(-\sin\theta\cos\theta + \sin\theta\cos\theta) \\ &= 0. \end{aligned} \tag{39}$$

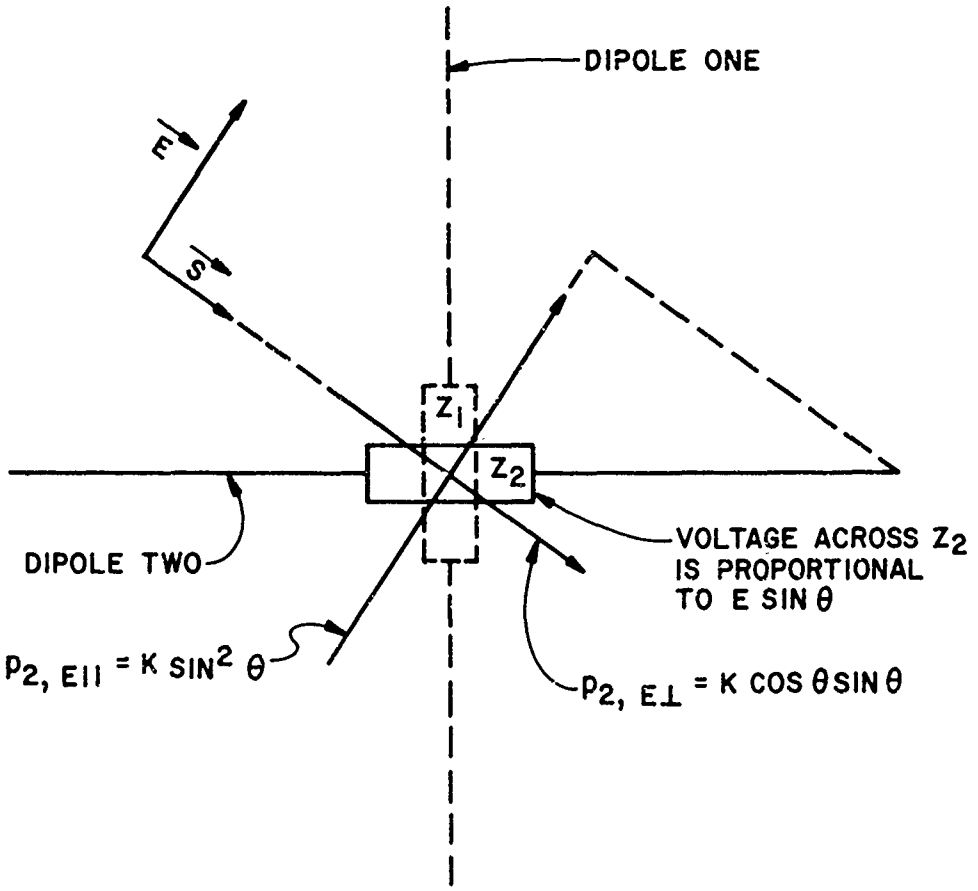

Figure 7. The dipole moment of dipole 2 can be resolved into components parallel and perpendicular to the incident electric field.

In summary, we see that the rather tedious arguments leading to equations (38) and (39) are consistent with the result of equation (37). Of course, as the length of the dipoles is increased, the simple trigonometric dependence for the current or charge distribution does not hold, and the polarization is not independent of the direction of the incident electric field.

2.4 Coupling of Scatterers

The dipole interaction of the scattering objects, each consisting of three mutually-perpendicular and centered, inductively-loaded dipoles, will be considered next. The starting point for the discussion of the coupling of scattering objects in both real and artificial dielectrics is the formula of Lorentz for the field within a hollow spherical cavity (centered at a particular molecule or scatterer) cut out of the dielectric

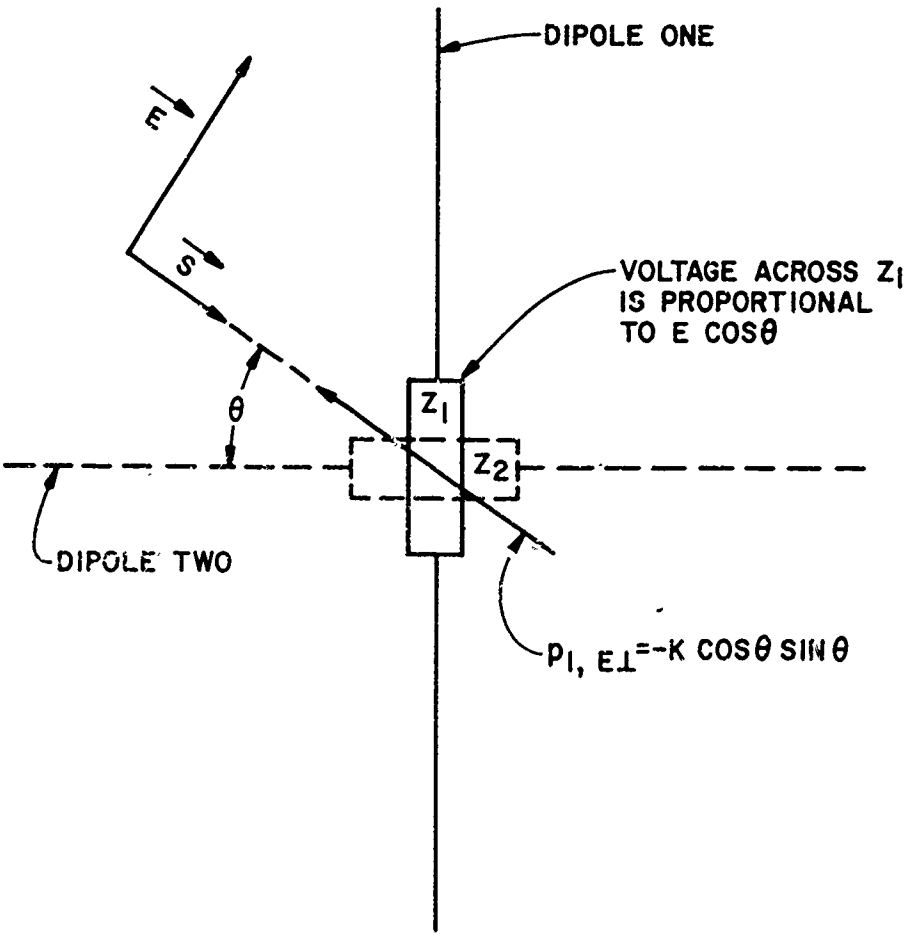

Figure 8. The vector $p_{1,E\perp}$ is the dipole moment component of dipole 1 that is perpendicular to the incident field.

(fig. 9). The displacement vector D normal to the dielectric surface between the sphere and the cavity must be continuous; therefore, the magnitude of P normal to the cavity surface equals the negative of the induced surface charge density σ_i. We may write $\sigma_i = -|\vec{P}| \cos\theta$. The field inside the cavity due to σ_i can be calculated at the center of the cavity with Coulomb's law:

$$E_s = \int_s \frac{\sigma_i \, ds \cos\theta}{4\pi \, \varepsilon_0 \, R^2}$$

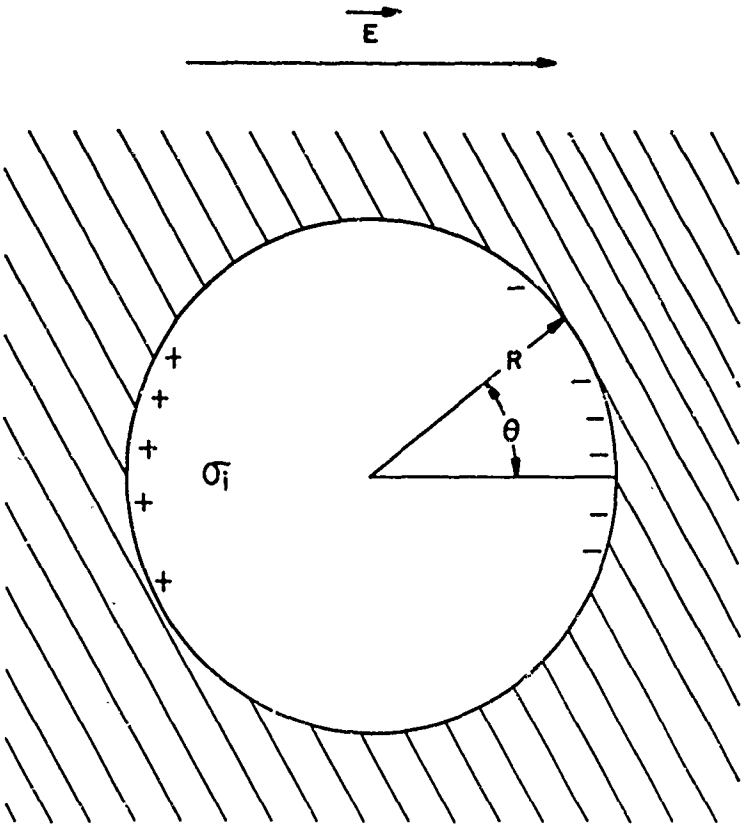

$$E_S = \int \frac{\sigma_i \, dS}{4\pi\varepsilon_0 R^2} \cos\theta$$

$$= \int_0^{\pi} \frac{|\vec{P}| \cos\theta}{4\pi\varepsilon_0 R^2} \cos\theta \, 2\pi R^2 \sin\theta \, d\theta$$

$$= \frac{|\vec{P}|}{3\varepsilon_0}$$

Figure 9. Spherical cavity in dielectric.

$$= \int_0^{\pi} \frac{|\vec{P}| \cos\theta \cos\theta \, 2\pi R^2 \sin\theta \, d\theta}{4\pi \varepsilon_0 R^2}$$

$$= \frac{|\vec{P}|}{2\varepsilon_0} \int_0^{\pi} \cos^2\theta \sin\theta \, d\theta$$

$$= \frac{|\vec{P}|}{3\varepsilon_0}.$$

Therefore, the local field at the center of the cavity at a particular molecule or scatterer is

$$\vec{E}_{loc} = \vec{E} + \frac{1}{3\varepsilon_0} \vec{P} + \vec{E}_2.$$

Here E is the ordinary macroscopic field, P is the polarization of the dielectric, and E_2 is the mean field due to the matter within the sphere itself (exclusive of the central scatterer). The magnitude of E_2 will depend on the distribution of scatterers within the spherical cavity. Lorentz showed that if the molecules are arranged in a cubical array, E_2 will be zero. Lorentz also indicated that to a certain degree of approximation $E_2 \simeq 0$ for such isotropic bodies as glass, fluids, and gases. We will discuss this approximation in a later section.

Assuming that $E_2 = 0$, we obtain the following value for the local field at a scatterer:

$$\vec{E}_{loc} = \vec{E} + \vec{P}/3\varepsilon_0 \tag{40}$$

The dipole moment of a scatterer is then $\vec{p} = \chi_{av3} \vec{E}_{loc}$, but,

$$\vec{P} = \vec{p} N = \chi_{av3} N \vec{E}_{loc}$$

where N is the number density of scatters per unit volume. According to the usual notation:

$$\varepsilon \vec{E} = \varepsilon_0 \vec{E} + \vec{P}.$$

Therefore

$$\vec{P} = \vec{E} (\varepsilon - \varepsilon_0)$$

and

$$\vec{P} = \chi_{av3} N \vec{E}_{loc} = \chi_{av3} N (\vec{E} + \vec{P}/3\varepsilon_0)$$

$$= \chi_{av3} N (\vec{E} + \frac{\vec{E}(\varepsilon_1 - \varepsilon_0)}{3\varepsilon_0}). \tag{41}$$

This is the Clausius-Mossotti relation. Equation (41) can be manipulated to yield:

$$\varepsilon = \varepsilon_o \frac{1 + 2 N \chi_{av3}/3\varepsilon_0}{1 - N \chi_{av3}/3\varepsilon_0}. \tag{42}$$

he above expression is only valid when the local electric field E_{loc} at a scattering obstacle can be expressed as

$$\vec{E}_{loc} = \vec{E} + \vec{P}/(3\varepsilon_0) \tag{43}$$

where E is the space average field inside the artificial dielectric.

The local fields for simple tetragonal and hexagonal lattices have also been calculated by a number of workers. Collin[7],[22] considers a three-dimensional array of y-directed unit dipoles at x = na, y = mb, and z = sc. He excludes the dipole at x = y = z = 0 and calculates the local field at x = y = z = 0. The potential due to a unit dipole at x_0, y_0, z_0 is

$$\phi = \frac{\hat{j} \cdot \vec{r}}{4\pi \varepsilon_0 r^3} \tag{44}$$

where $r = \left[(x - x_0)^2 + (y - y_0)^2 + (Z - Z_0)^2\right]^{1/2}$. For the array of y-directed dipoles we then have (fig. 10)

$$\phi = \frac{1}{4\pi\varepsilon_0} \sum_{n=-\infty}^{\infty} \sum_{s=-\infty}^{\infty} \sum_{m=-\infty}^{\infty}{}' \frac{y - mb}{\left[(x-na)^2+(y-mb)^2+(Z-sc)^2\right]^{3/2}} \tag{45}$$

where the prime indicates the omission of the n = m = s = 0 term. The effective polarizing field at x = 0, y = 0, z = 0 will then be E + E_i, where E is the external applied field and where

$$E_i = -\frac{\partial \phi}{\partial y}\Big|_{x = y = z = 0}$$

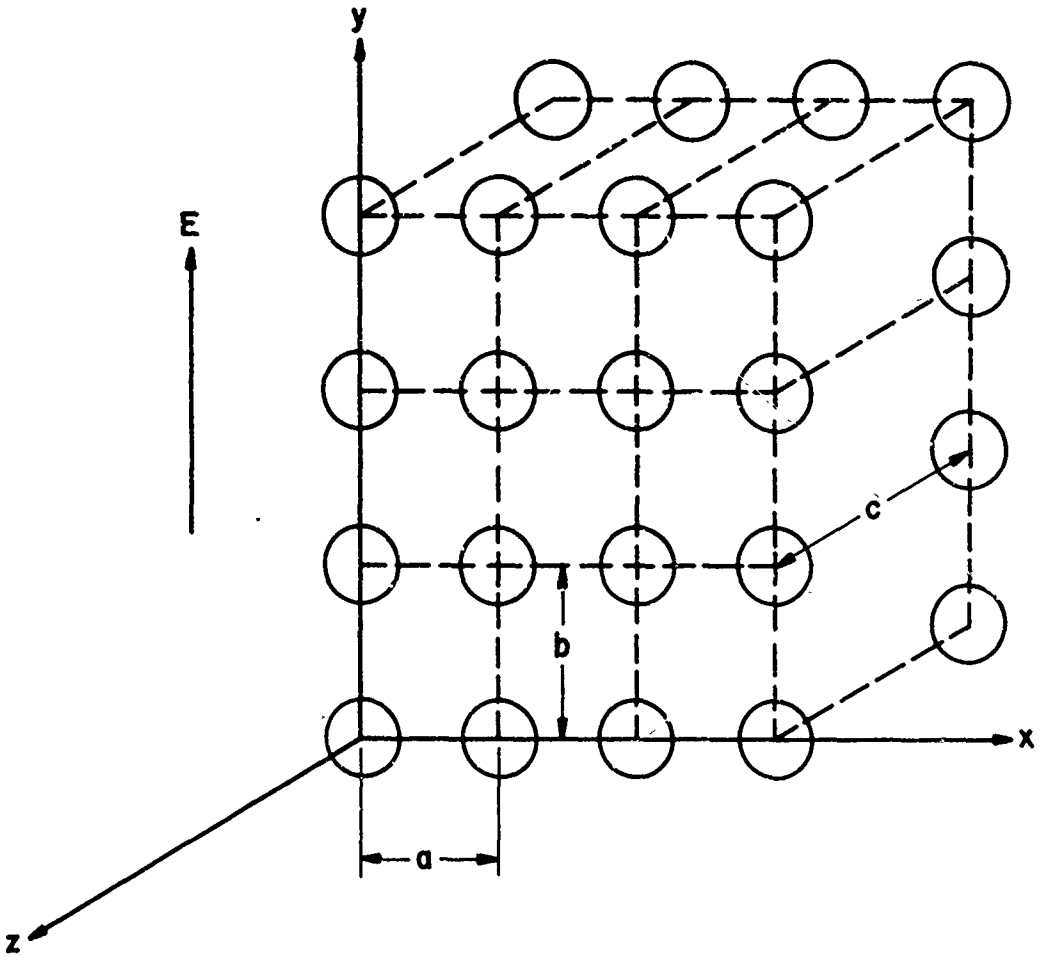

CUBIC LATTICE $a = b = c$

TETRAGONAL LATTICE $a = c \neq b$

HEXAGONAL LATTICE $a \neq b \neq c$

Figure 10. Three-dimensional array of inductively-loaded dipoles enclosed in styrofoam spheres.

$$= \frac{1}{4\pi\varepsilon_0} \sum_{m=-\infty}^{\infty} \sum_{n=-\infty}^{\infty} \sum_{s=-\infty}^{\infty} \frac{2(mb)^2-(na)^2-(sc)^2}{\left[(mb)^2+(na)^2+(sc)^2\right]^{5/2}}. \qquad (46)$$

Note that the above expression is not only evaluated inside the Clausius-Mossotti sphere, but over all space. We therefore do not have to consider a contribution from the inside surface of the sphere.

Collin evaluates expression (46) and obtains

$$E_i = \frac{1}{\varepsilon_0}\left\{\frac{1.201}{\pi b^3} - \frac{8\pi}{b^3}\left[K_0\left(\frac{2\pi c}{b}\right) + K_0\left(\frac{2\pi a}{b}\right)\right]\right\} \qquad (47)$$

where K_0 is the so-called modified Bessel function of order zero. Equation (47) is for unit dipoles. In our case of inductively-loaded dipoles we would have

$$E_i = \frac{1}{\varepsilon_0}\left\{\frac{1.201}{\pi b^3} - \frac{8\pi}{b^3}\left[K_0\left(\frac{2\pi c}{b}\right) + K_0\left(\frac{2\pi a}{b}\right)\right]\right\} \chi_{av3} \qquad (48)$$

or

$$E_{loc} = E + \frac{1}{\varepsilon_0}\left\{\frac{1.201}{\pi b^3} - \frac{8\pi}{b^3}\left[K_0\left(\frac{2\pi c}{b}\right) + K_0\left(\frac{2\pi a}{b}\right)\right]\right\}\left(\frac{j B^2}{4\omega(j\omega L+Z_{22})}\right). \qquad (49)$$

The above equation corresponds to a cubic lattice if a = b = c, a tetragonal lattice if only two of the quantities are equal, and a hexagonal lattice if none of the quantities, a, b, or c are equal. In the case of the cubic lattice we find that

$$E_{loc} = E + \frac{1.06\ N}{\pi\ \varepsilon_0}\chi_{av3} \qquad (50)$$

and, therefore

$$\varepsilon = \varepsilon_0 \frac{1 + \frac{2.08}{\pi}\frac{N}{\varepsilon_0}\chi_{av3}}{1 - \frac{1.06}{\pi}\frac{N}{\varepsilon_0}\chi_{av3}} \qquad (51)$$

which is to be compared with equation (42).

2.5 Deviations from the Clausius-Mossotti Equation Due to Randomness of Scatterers

J.K. Kirkwood[23,24] has calculated the deviations that one might expect from equation (40) in the case of a random distribution of molecules consisting of hard spheres. Specifically, Kirkwood considered a molecular interaction potential of the form

$$\begin{aligned} W(r) &= \infty \qquad 0 \leq r \leq a \\ &= 0 \qquad r > a \end{aligned} \tag{52}$$

where a is the diameter of a molecule.

Kirkwood's model is not wholly applicable to an artificial dielectric formed by dumping spherical scatterers into a container because the scatterers do not necessarily assume a completely random distribution. For example, depending, among other factors, on how smooth they are, the spheres can arrange themselves into various specific lattices or combinations of lattices. The different lattices can even correspond to different dipole number densities.

It is interesting to note that statistical mechanical averaging based on the molecular interaction equation (52) yields a value of the permittivity that is not a function of the thermodynamic temperature T. This follows because the value of the exponential term $\exp[-W(r)/kT]$ is either 0 or 1. In a gas or fluid the averaging can be over time; in our static collection of scattering dipoles the averaging would have to be over an ensemble of different containers each filled with a aggregation of spherical dipole scatterers. Kirkwood's approach can be summarized as follows: As in the lattice case, the local field is obtained by summing over the potentials due to individual dipoles. We can say that the effective polarizing field E_{loci} at scatterer i will be given by $E + E_i$, where E is the external applied field and E_i is given by the sum over N individual dipoles:

$$\vec{E}_i = - \sum_{\substack{k=1 \\ \neq i}}^{N} \underline{\underline{T}}_{ik} \cdot \vec{P}_k \tag{53}$$

where the dipole-interaction dyadic is given by

$$\underline{\underline{T}}_{ik} = \frac{1}{4\pi\varepsilon_0} \frac{1}{r_{ik}^3} \left[\underline{\underline{I}} - 3 \frac{\vec{r}_{ik}\,\vec{r}_{ik}}{r_{ik}^2} \right] \tag{54}$$

The polarization of an individual scatterer is given by

$$\vec{p}_i = \varepsilon_0 \underline{\underline{\alpha}} \cdot \vec{E}_{loci} = \varepsilon_0 \underline{\underline{\alpha}} \cdot (\vec{E} + \vec{E}_i)$$

$$= \varepsilon_0 \alpha \vec{E} - \varepsilon_0 \alpha \Sigma \underline{\underline{T}}_{ik} \cdot \vec{p}_k \tag{55}$$

We therefore have N simultaneous equations

$$\vec{p}_i + \alpha\varepsilon_0 \Sigma \underline{\underline{T}}_{ik} \cdot \vec{p}_k = \alpha\varepsilon_0 \vec{E} \quad i = 1, \ldots N$$

that would have to be solved in order to obtain E_{loci} for each of the individual scatterers in the distribution of N scatterers in volume V. We can average the N equations and obtain

$$\bar{\vec{p}} + \alpha\varepsilon_0 \Sigma \overline{\underline{\underline{T}}_{ik} \cdot \vec{p}_k} = \alpha\varepsilon_0 \vec{E} \tag{56}$$

Kirkwood[23,24] incorporated the following fluctuation term

$$\vec{n} = \sum_{\substack{i=1 \\ i \neq k}}^{N} \left(\overline{\underline{\underline{T}}_{ik} \cdot \vec{p}_k} - \bar{\underline{\underline{T}}}_{ik} \cdot \bar{\vec{p}}_k \right) \tag{57}$$

and obtained

$$\bar{\vec{p}} + \alpha\varepsilon_0 \Sigma \bar{\underline{\underline{T}}}_{ik} \cdot \bar{\vec{p}} + \vec{n}\alpha\varepsilon_0 = \alpha\varepsilon_0 \vec{E} \tag{58}$$

If we can assume that

$$\overline{\underline{\underline{T}}_{12} \cdot \vec{p}_1} = \bar{\underline{\underline{T}}}_{12} \cdot \bar{\vec{p}}_1 \tag{59}$$

the fluctuation $\vec{n}$ is equal to zero and

$$\bar{\vec{p}} + \alpha\varepsilon_0 \bar{\vec{p}} \cdot \Sigma \bar{\underline{\underline{T}}}_{ik} = \alpha\varepsilon_0 \vec{E}. \tag{60}$$

Converting to the equivalent scalar equation we obtain:

$$\bar{p} = \frac{\alpha\varepsilon_0 E}{1 + \alpha\varepsilon_0 (\Sigma \bar{T}_{ik})}, \tag{61}$$

and

$$D = \varepsilon E = \varepsilon_0 E + P \tag{62}$$

$$= \varepsilon_0 E + \frac{N}{v}\overline{p}$$

$$= \varepsilon_0 E + \frac{\varepsilon_0 \frac{N}{v} \alpha E}{1 + \alpha \varepsilon_0 (\Sigma T_{ik})}. \tag{63}$$

The dipole interaction term can be averaged over the volume v to yield:

$$\Sigma \overline{T}_{ik} = -\frac{1}{3}\frac{N}{v}, \tag{64}$$

also

$$\alpha = \frac{\chi_{av3}}{\varepsilon_0} \tag{65}$$

and therefore

$$\varepsilon = \varepsilon_0 \left\{ 1 + \frac{\frac{N}{v}\alpha}{1 - 1/3 \frac{N}{v}\alpha} \right\} \tag{66}$$

or

$$\varepsilon = \varepsilon_0 \frac{1 + \frac{2}{3}\frac{N}{v}\frac{\chi_{av3}}{\varepsilon_0}}{1 - \frac{1}{3}\frac{N}{v}\frac{\chi_{av3}}{\varepsilon_0}}. \tag{67}$$

Equation (67) is to be compared with equations (51) and (42). After considerable mathematical manipulation and a number of approximations, Kirkwood managed to evaluate equation (57) for a substance consisting of a random distribution of hard noninteracting spheres of diameter a:

$$n \simeq \left(\frac{1}{9b} - \frac{5}{48v}\right) \frac{N^2 \alpha^2 D}{v} \tag{68}$$

where

$$b = \frac{2\pi N a^3}{3} = 4N\left(\frac{\pi a^3}{6}\right)$$

$$= 4 \text{ (volume of spherical scatterers)}.$$

To obtain a rough estimate of the validity of using the Clausius-Mossotti equation for a random distribution of styrofoam ball dipole scatterers, we can compare the value of n given by equation (68) with the value of [23]

$$1 - \alpha \Sigma T_{ik} = 1 + \frac{1}{3}\frac{N\alpha}{v}$$

For the experimental situation discussed in Section 2:

$$\frac{n}{1 - \alpha \Sigma T_{ik}} = .22$$

and we might expect the Clausius-Mossotti equation to be a reasonable first approximation. Actually, as we have pointed out, Kirkwood's statistical model is not necessarily applicable to our aggregation of dipole scatterers because the dipole scatterers in the artificial dielectric do not necessarily assume a random distribution. The validity of the Clausius-Mossotti equation as applied to our artificial dielectric should really be tested empirically.

3. COMPARISON OF EXPERIMENT WITH THEORY

In order to orient ourselves in regard to the parameters such as the dipole load impedance and Z_{22} we will use equations (36) and (42) to design an artificial dielectric with some actual experiments in mind. The frequency range considered will be dictated by the band pass characteristics of the type 2300 waveguide. The type 2300 waveguide, the largest standard waveguide, has internal dimensions of 23.0 x 11.5 in., a lower cutoff frequency of 2.56×10^8 H, and a recommended upper frequency limit of 4.9×10^8 H. The frequencies in this range are much higher than the values usually quoted for nuclear EMP pulses, but we will consider designing an artificial dielectric to operate at these high frequencies because of the convenience of using waveguide techniques in measuring the properties of an artificial dielectric.

Let us concider the following series of parameters as an orientation exercise. We begin with an artificial dielectric constructed out of scatterers consisting of three mutually-perpendicular inductively-loaded 7-in. long dipoles loaded with a number of different values of inductance. Let the dipole stems have a radius of 0.1 cm. We choose the density of

scatterers to be 264 per cubic meter. This density corresponds to an aggregation of 48 scatterers distributed throughout a rectangular container with dimensions 23 x 11.5 x 41.5 in. Equations (36) and (42) can be employed to calculate the dielectric constant of the artificial dielectric as a function of frequency in the band-pass region of the type 2300 waveguide. Figure 11 shows values of the real part of the permittivity calculated with equations (36) and (42) for a frequency range between 300 and 500 MH. The four curves correspond to dipole load inductances of 0.4, 0.6, 0.9, and 1.4 μH. The magnitude of the radiation resistance of the dipoles is very small compared to the values of the magnitude of the inductive loads; therefore, the imaginary components of the permittivity are very small.

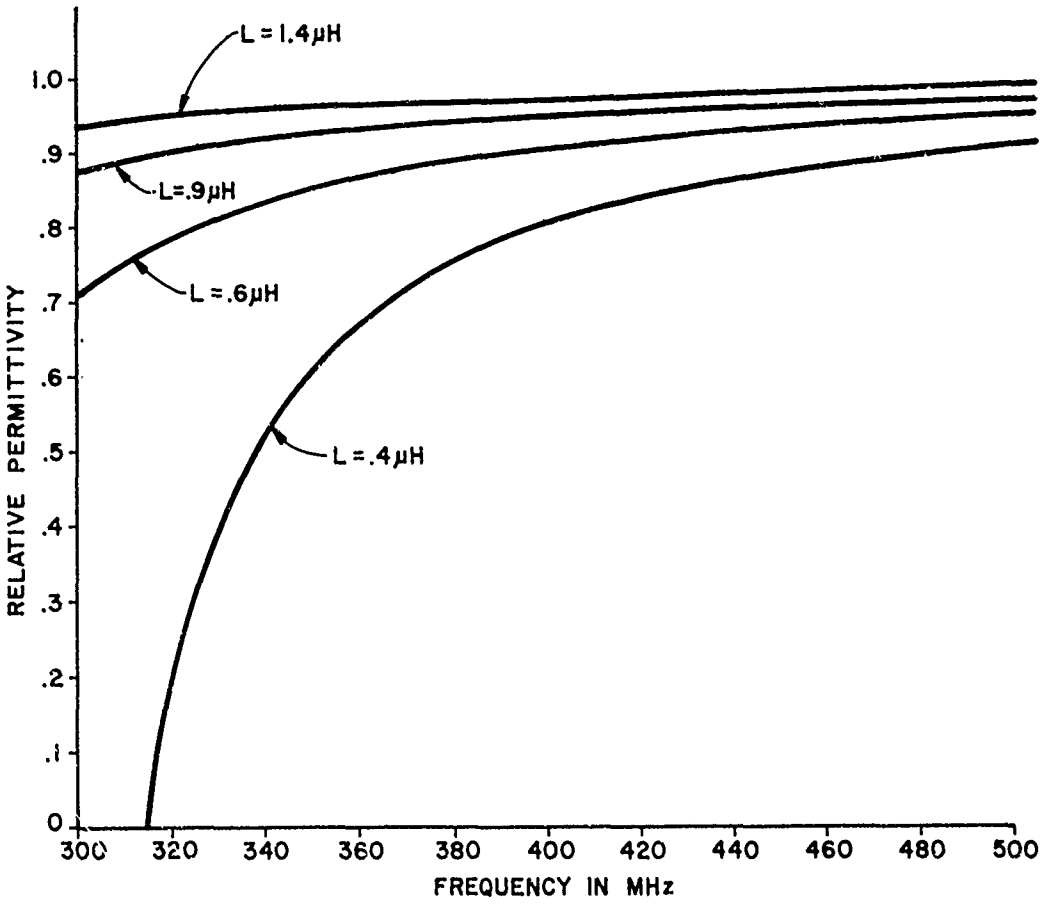

Figure 11. Values of relative permittivity calculated with equations (36) and (42) for a number of different inductive loads. The other parameters are discussed in the text.

If we want to model a Lorentz plasma in which the electrons have a collision frequency $\nu \neq 0$, the load impedance of our dipoles must have a resistive component. Equation (36) then becomes:

$$X_{av3} = \frac{-j B^2}{4\omega(j\omega L + R + Z_{22})} \tag{69}$$

where R is the value of the resistance. In figures 12a to 12d we present values of the real part of the permittivity calculated with equations (69) and (42) with L = 0.4 μH. The series of four figures shows the effect of different values of the resistive component R on the magnitude of the resonance occurring when $j\omega L = Z_{22}$. Figure 12a, corresponding to a purely inductive load, emphasizes the resonance behavior of the artificial dielectric produced when the load inductance L is in resonance with the capacitive impedance of the dipole. As can be expected the Q of the resonance is reduced by including a resistance in the dipole load impedance.

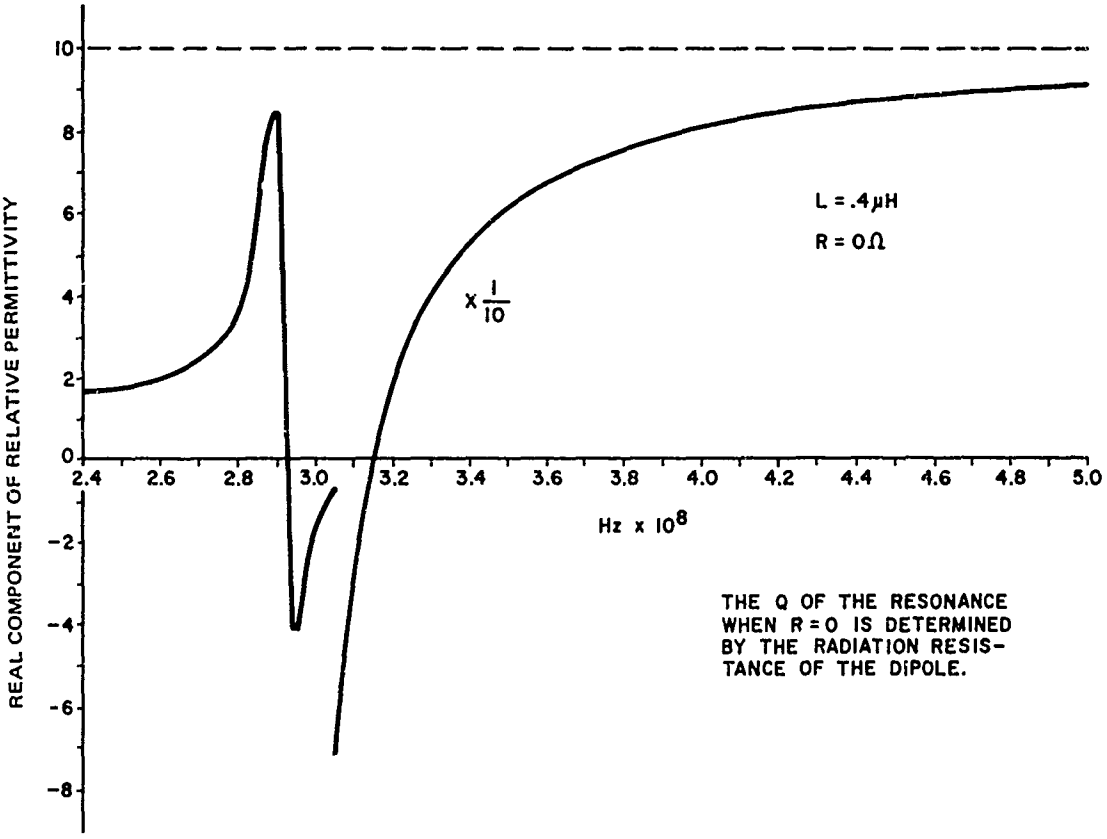

Figure 12a. The real component of relative permittivity calculated with equations (69) and (42). The value used for L is .4 μH and the value used for R is 0Ω. The other parameters are the same as those employed to obtain figure 11.

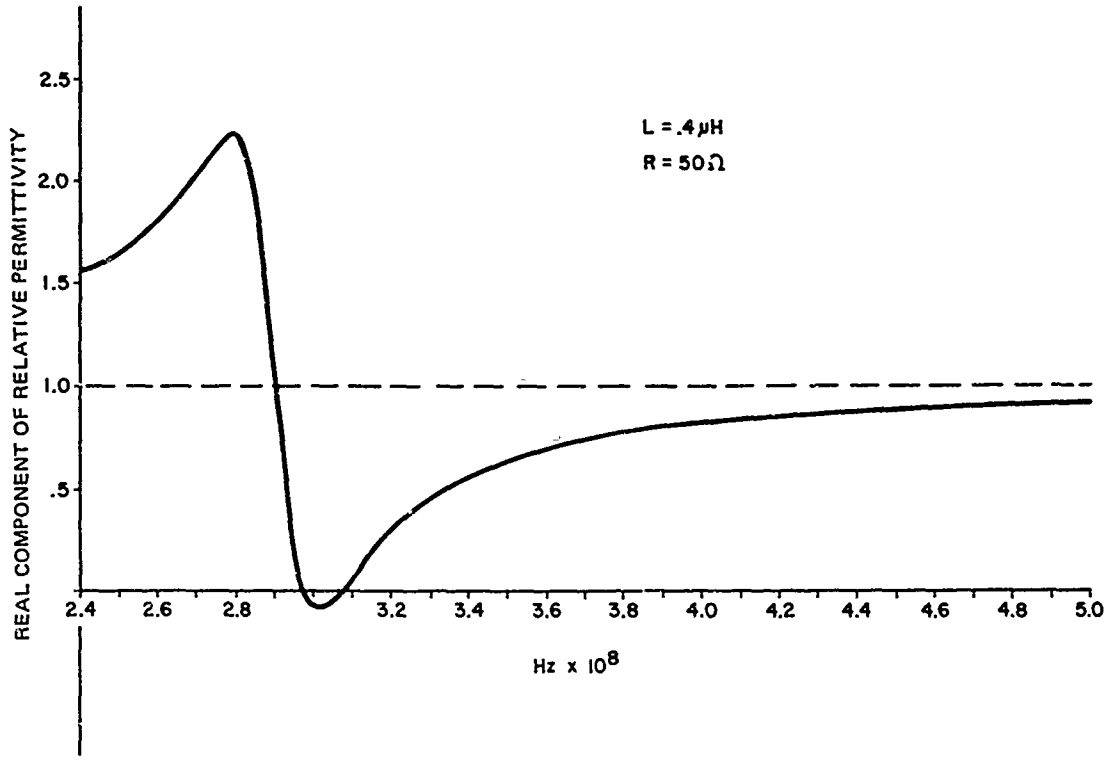

Figure 12b. The real component of relative permittivity calculates with equations (69) and (42). The value used for L is .4 μH and the value used for R is 50Ω. The other parameters are the same as those employed to obtain figure 11.

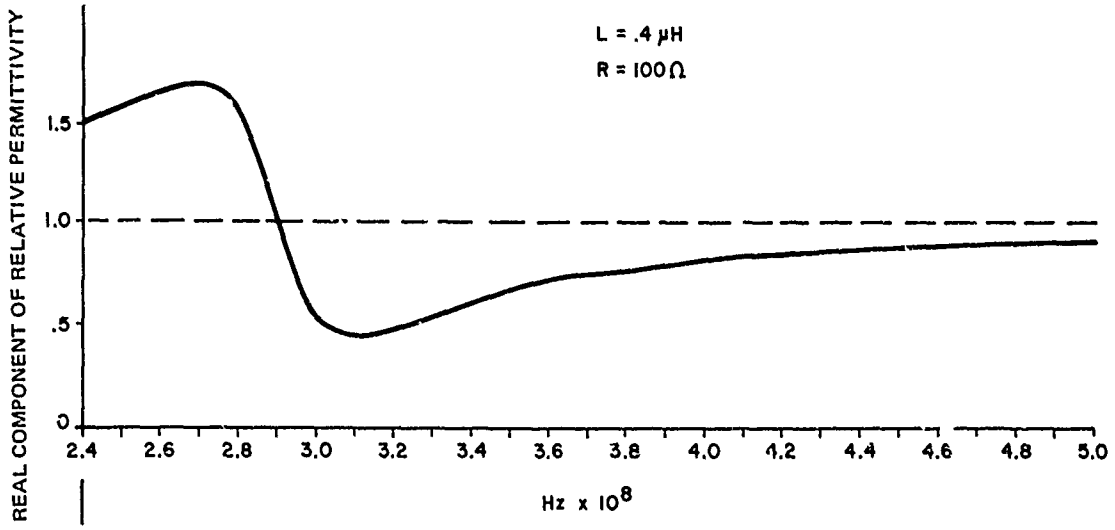

Figure 12c. The real component of relative permittivity calculated with equations (69) and (42). The value used for L is .4 μH and the value used for R is 100Ω. The other parameters are the same as those employed to obtain figure 11.

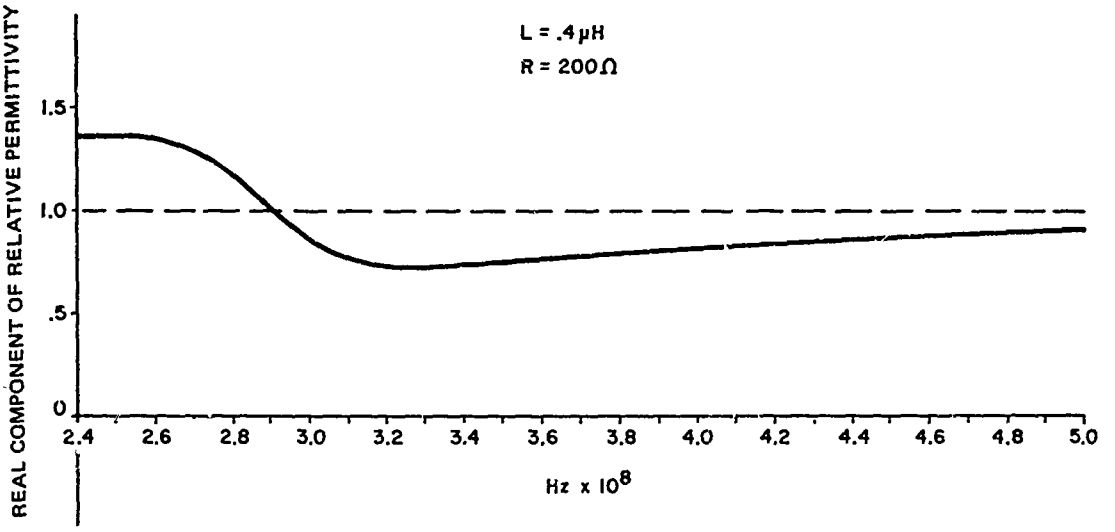

Figure 12d. The real component of relative permittivity calculated with equations (69) and (42). The value used for L is .4 μH and the value used for R is 200Ω. The other parameters are the same as those employed to obtain figure 11.

In our first experiment we searched for the resonance predicted by equation (36) and shown in figure 12a. The experimental technique[25] was straightforward and is depicted in figure 13. The ratio of the incident electric field E_I to the reflected electric field E_R was obtained by measuring the standing wave ratio with a slotted line. The artificial dielectric sample shown in figure 13 consists of an aggregation of 48 of our 7 in. styrofoam balls each containing 3 mutually-perpendicular dipoles. The balls were enclosed in a rectangular box measuring 23 x 11.5 x 41.5 in. The results of the experiment are shown in figure 14. It is comforting to note that there is a large reflection at approximately the frequency of the resonance shown in figure 12a.

In a second series of experiments we measured the permittivity of our artificial dielectric utilizing the well-known shorted waveguide technique described in great detail by von Hippel[26]. Very briefly, the technique consists of measuring the null point of a standing wave in a shorted waveguide. A sample of length ℓ is then inserted into the shorted waveguide and the shift in the standing wave null is noted. The index of refraction of the dielectric sample of length ℓ can then be calculated in terms of ℓ and the shift in the standing wave null point.

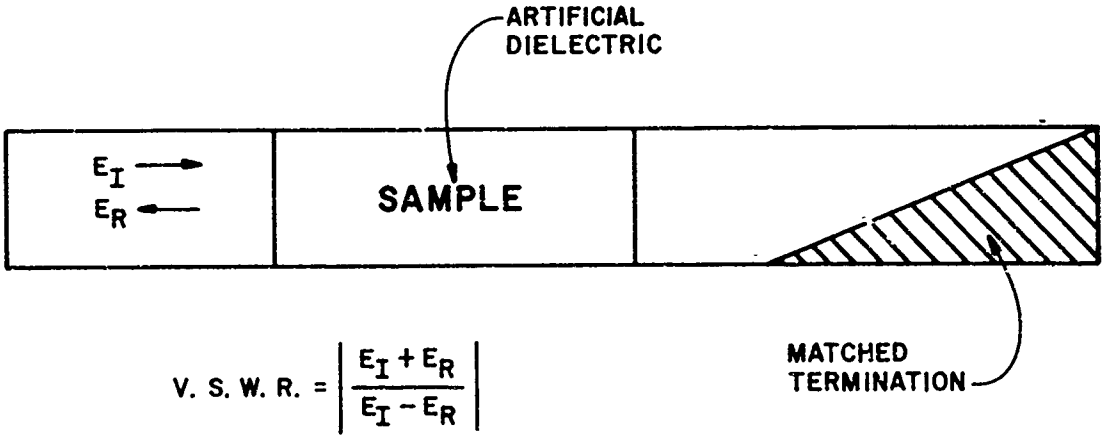

Figure 13. Experimental setup used in determining the resonance frequency of the artificial dielectric. The sample consisted of 48 scatterers or "molecules." The V.S.W.R. or voltage standing-wave ratio was determined with a slotted line.

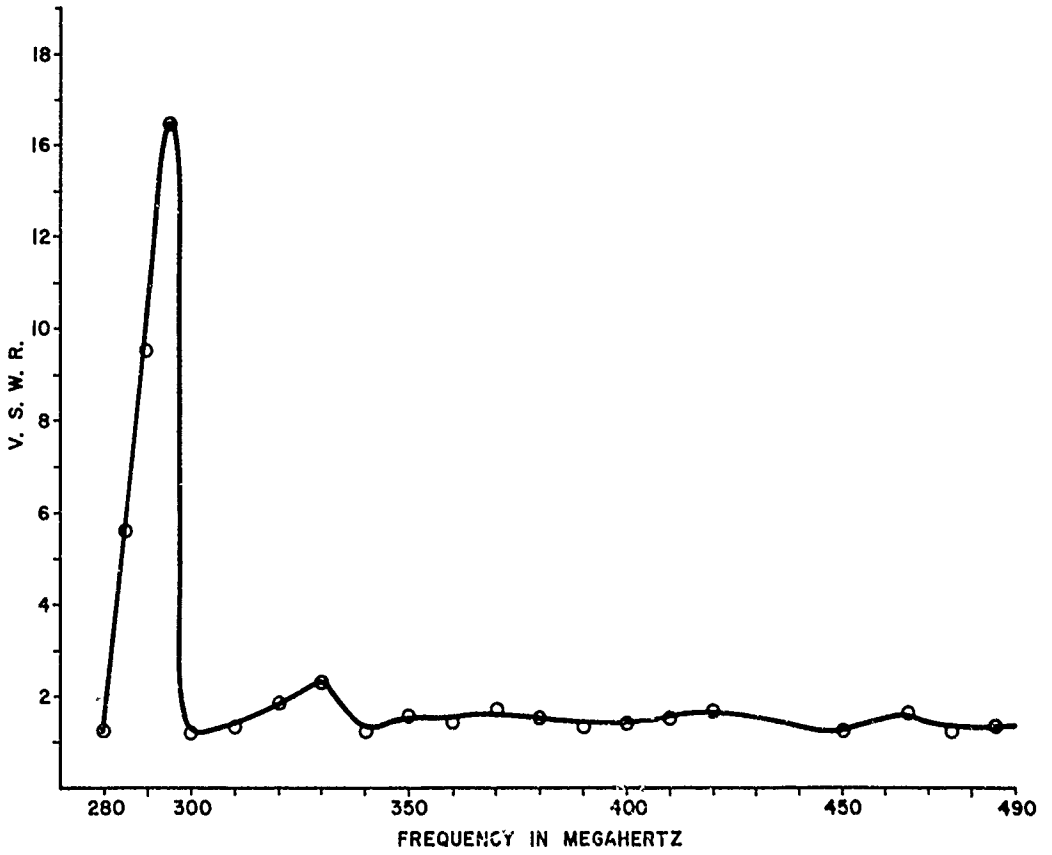

Figure 14. Experimental standing-wave ratio corresponding to the setup shown in figure 13.

Our experimental values of the index of refraction and some calculated values are shown in figure 15. The measurements were of two different artificial dielectric sample sizes; one sample consisted of an aggregation of 24 scatterers measuring 23 x 11.5 x 20.75 in. in volume. The length of the sample was, ℓ = 20.75 in. The other sample consisted of an aggregation of 48 scatterers in a rectangular volume measuring 13 x 11.5 x 41.5 in In this case, ℓ = 41.5 in.

The difference between the theoretical index of refraction curve corresponding to L = 0.4 μH and R = 0 and the measured index of refraction is about 30 percent. A possible source of the disparity between experiment and theory is that we used the dimension of the cardboard box that enclosed the scatterers to obtain ℓ. The effective length of the very granular artificial dielectric sample is most probably not the size of the box containing the scatterers. The boundary of our artificial dielectric is somewhat nebulous and needs more study.

Further experimental measurements of the electromagnetic characteristics of our inductively-loaded dipoles are now under consideration. These new measurements would involve the irradiation of a monopole that is immersed in an expanse of artificial dielectric medium. The new experimental approach would overcome the limitations imposed by the relatively small size and narrow frequency band pass of a waveguide. The measurements could also be carried out at lower frequencies which are closer to the actual nuclear EMP spectrum. As the frequency is lowered, the size of the scatterer compared to the wavelength would decrease. That is to say, the artificial dielectric would have less granularity and the boundary of the artificial dielectric would become more well defined.

If we construct a cylindrical monopole of height H it would have a resonance or maximum skin current at frequency f given by

$$f = \frac{4H}{\pi c}.$$

If the monopole were then submerged into an artificial dielectric with an index of refraction n, the resonance of the monopole would change to

$$f = \frac{4H}{\pi c} n.$$

The influence of the artificial dielectric of the resonance characteristics and skin currents of other shapes such as a sphere could also be studied.

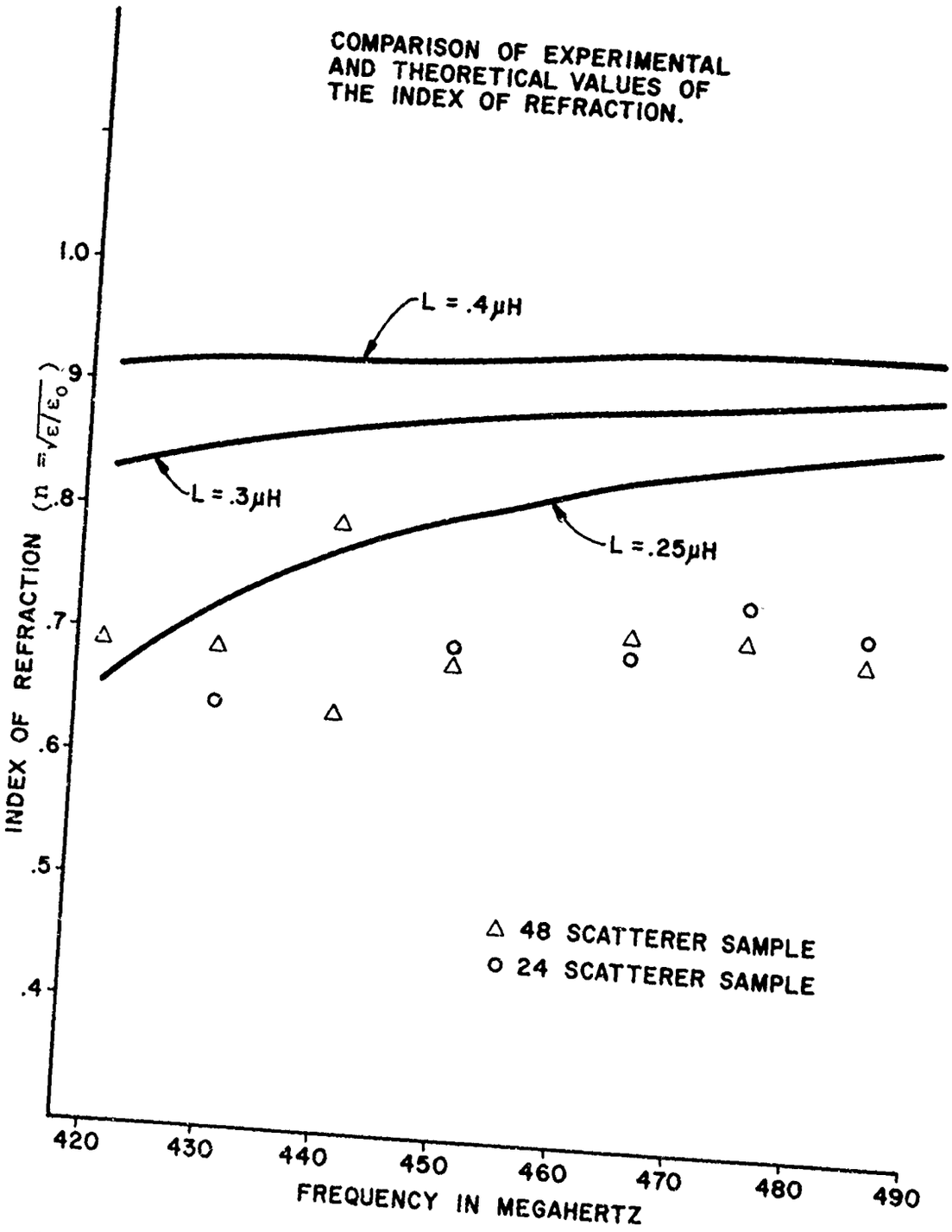

Figure 15. The accuracy of the experimental points is limited by the granularity of the sample and the corresponding indefiniteness of the sample edges.

4. SUMMARY AND CONCLUSIONS

We first introduced a simple quasi-static model of the artificial dielectric consisting of inductively-loaded dipoles which (1) ignored the dipole capacitance, and (2) assumed that the dipole-dipole interaction could be neglected. These two simplifying assumptions yielded an expression for the permittivity of the artificial dielectric that behaved in a manner surprisingly analogous to the permittivity of a simple Lorentzian plasma. It was noted that the granularity of fluctuations of the artificial dielectric could be decreased by constructing the dipole scatterers out of three mutually-perpendicular scatterers.

Then the effect of the capacitance of the inductively-loaded dipole scatterers was examined and limits set on the assumption that the inductance dominated the behavior of the inductively-loaded dipole. Next, the effect of dipole-dipole interactions on the artificial dielectric was considered. A relatively rigorous expression for a cubic, tetragonal or hexagonal lattice was obtained. An estimate of the effect of a random distribution of scatterers on the value of the permittivity predicted by equation (42) was also obtained.

It is interesting that the more exact expressions for the dielectric constant of the artificial dielectric, which considered both the effect of the capacitive dipole impedance and the dipole-dipole interaction, did not model the behavior of a Lorentzian plasma as well as the original simplified approach. Nevertheless, the artificial dielectric did have an index of refraction less than one over a relatively broad spectrum. We are now looking into the possibility of improving correspondence between the frequency dependence of our artificial dielectric and a Lorentzian plasma. The approach being investigated is based on the substitution of a more complicated one-terminal pair in place of the simple inductive dipole load used in our present scatterers. By synthesizing a suitable one-terminal pair out of a number of lumped impedances we hope to improve the correspondence between the frequency dependence of the artificial dielectric and a Lorentz plasma.

The experimental examination of the theoretical expressions for the dielectric constant of our artificial dielectric was constrained by the dimensions and frequency characteristics of available waveguide equipment. The predictions of equations (36) and (42) for the dielectric constant of the artificial dielectric were found to be in fair agreement with experimental results.

REFERENCES

1. M.A. Heald and C.B. Wharton, Plasma Diagnostics with Microwave, John Wiley and Sons, Inc., New York, 1965, p. 6.

2. W. Rotman, "Plasma Simulation by Artificial Dielectric and Parallel-plate Media," IRE Transactions on Antennas and Propagation, Vol. AP-13, p. 587, July 1965.

3. W.E. Koch, "Metallic Delay Lenses," Bell System Technical Journal, Vol. 27, pp. 58-82, January 1948.

4. J. Brown, "Microwave Lenses," Methuen and Co., Ltd., London, 1953.

5. H. Jasik, Antenna Engineering, McGraw-Hill Book Co., New York, 1963, Section 14.6. Schelkunoff and Friis, Antennas Theory and Practice, John Wiley and Sons, Inc., New York, 1952, p.577.

6. R.W. Corkum, "Isotropic Artificial Dielectrics," Proc. IRE, Vol. 40, pp. 574-587, May 1952.

7. M.M.Z. El-Kharadly and W. Jackson, "The Properties of Artificial Dielectrics Comprising Arrays of Conducting Particles," Proc. IEE (London), Vol. 100, Part III, pp. 199-212, July, 1953.

8. K.E. Golden, "Simulation of a Thin Plasma Sheath by a Plane of Wires," IRE Transactions on Antennas and Propagation, Vol. AP-13, p. 587, July 1965.

9. J. Brown, "Artificial Dielectrics Having Refractive Indices Less than Unity," Proc. IEE, Monograph No. 62R, Vol. 100, p. 51.

10. M.M.Z. El-Kharadly, "Some Experiments on Artificial Dielectrics at Centimetre Wavelengths," Proc. IEE, Paper No. 1700, Vol. 102B, p. 22, January 1955.

11. L. Brillouin, Wave Propagation in Periodic Structures, McGraw-Hill, New York, 1946.

12. J.C. Slater, Microwave Electronics, D. Van Nostrand Co., New York, 1950.

13. H.S. Bennett, "The Electromagnetic Transmission Characteristics of Two Dimensional Lattice Medium," J. Appl. Phys., Vol. 24, pp. 785-810, June 1953.

14. P.J. Crepeau and P.R. McIsaac, "Consequences of Symmetry in Periodic Structures," Proc. IEE, January 1964, p. 33.

15. R. F. Harrington, "Small Resonant Scatterers and Their Use for Field Measurements," IRE Transactions of Microwave Theory and Techniques, May 1962, pp. 165-174.

16. V.H. Ramsey, "The Reaction Concept in Electromagnetic Theory," Phys. Rev. Ser. 2, 94, No. 6, pp. 1483-1491, June 15, 1954.

17. R.F. Harrington, Time-Harmonic Electromagnetic Fields, McGraw-Hill Book Co., New York, 1961, Section 7-9.

18. R.W.P. King, The Theory of Linear Antennas, Harvard University Press, Cambridge, Mass., 1956, p. 184.

19. Ibid., p. 470.

20. R.W.P. King, R.B. Mack, and S.S. Sandler, Arrays of Cylindrical Dipoles, Harvard University Press, Cambridge, Mass., p. 359, Formula 8.87, 887.

21. J.H. Richmond, "Coupled Linear Antennas with Skew Orientation," IEEE Transactions on Antennas and Propagation, Vol. AP-18, No. 5, September 1970, pp. 694-696.

22. R.E. Collin, Field Theory of Guided Waves, McGraw-Hill Book Co., New York, 1960, p. 517.

23. J.G. Kirkwood, "On the Theory of Dielectric Polarization," J. Chem. Phys., Vol. 6, p. 592, September 1936.

24. J.G. Kirkwood, "The Local Field in Dielectrics," Annals of the New York Academy of Sciences, Vol. XL, Article 5, p. 315.

25. E.L. Ginston, Microwave Measurements, McGraw-Hill, New York, 1959, p. 235.

26. A.R. von Hippel, Editor, Dielectric Materials and Applications, The M.I.T. Press, Cambridge, Mass., 1954, Section 2, p. 63, by William B. Westphal.